2008 Water Reactor Fuel Performance Meeting
October 19~23, 2008, Renaissance Seoul Hotel, Seoul, Korea
www.wrfpm2008.org
Paper No. 8070

FRACTURE MECHANICS APPROACH FOR FAILURE MODE ANALYSIS IN CABRI AND NSRR RIA TESTS

Vincent Georgenthum[1], Tomoyuki Sugiyama[2], Yutaka Udagawa[2], Toyoshi Fuketa[2], Jean Desquines[1]

1: Institut de Radioprotection et de Sûreté Nucléaire
Direction de la Prévention des Accidents Majeurs
BP3 13115 Saint-Paul-Lez-Durance Cedex, France
Tel: +33 (0)4 42 19 95 36, Fax:+33 (0) 4 42 19 91 66 , email: vincent.georgenthum@irsn.fr

2: Japan Atomic Energy Agency
Nuclear Safety Research Center
Tokai Mura, Naka-Gun Ibaraki-ken, 319-1195, Japan
Tel:+81-29-282-5955, Fax:+81-29-282-5429, email: sugiyama.tomoyuki@jaea.go.jp

Abstract *– A survey of failure conditions of fuel rods submitted to RIA transient has been conducted on NSRR and CABRI tested rods. This survey highlighted the impact of hydride content and distribution on cladding failure and also a slightly different rod behaviour in these two experimental facilities. An Elastic Plastic Fracture Mechanics approach has been derived in order to better understand the failure conditions of the cladding during the Pellet Cladding Mechanical Interaction (PCMI) phase of a RIA transient. The deleterious impact of incipient cracks versus fuel averaged enthalpy has been evaluated through the calculation of the Rice integral (or J-integral).*
The J-integral is evaluated in a module coupled with the SCANAIR code and compared to the critical value of the J-integral (Jc) deduced from the fracture toughness (K_{Ic}) of Zircaloy based on a literature review. This approach allows to calculate, at each time during the PCMI phase, the incipient crack that would lead to the failure of the cladding. An analysis of the clad metallographic examination performed on CABRI an NSRR tested fuel rods has been done to determine the depth of the brittle zone, that is to say the length of incipient crack in each rod.
This analysis shows that during the PCMI phase the J-integral can be used both in the elastic and elasto-plastic ranges to predict the failure occurrences.
The study also points out that due to the strong dependence of hydride solubility with temperature, the conditions are more severe in the NSRR room temperature conditions than in the CABRI or the Pressurized Water Reactor ones (280°C). The incipient crack depth to be considered in PWR conditions corresponds to the outer hydride rim depth in the cladding, that is correlated with the cladding corrosion level represented by outer zirconia layer thickness. This failure prediction improvement will contribute to a physically based definition of a RIA failure criteria.

I. INTRODUCTION

In the frame of their research programs on high burnup fuel safety, the French Institut de Radioprotection et de Sûreté Nucléaire (IRSN) and the Japan Atomic Energy Agency (JAEA) performed a large set of tests respectively in the CABRI reactor ([1], [2]) and in the Nuclear Safety Research Reactor (NSRR, [3], [4], [5], [6]). These tests devoted to the study of PWR fuel rod behavior during Reactivity Initiated Accident (RIA) evidenced the increase of Zircaloy cladding brittleness with burnup, especially over an average fuel burnup of about 40 GWd/tM. The maximal fuel enthalpy during the test (for non failed tests) or at failure (for failed tests) have been gathered on Fig. 1.

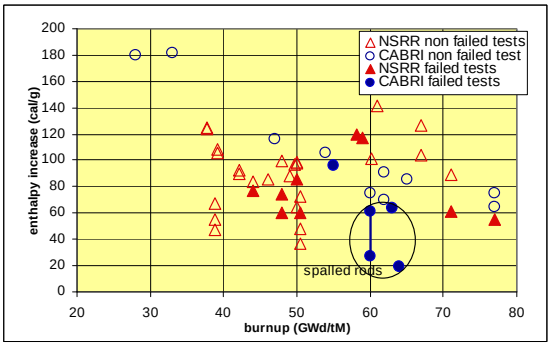

Fig. 1: maximal fuel enthalpy or enthalpy at failure for PWR test performed in NSRR and CABRI reactors.

Nevertheless, the results also show that the decrease of the failure limit is not only linked to the fuel burnup increase. It is now fully accepted that the main reason of this embrittlement is the hydrogen absorbed with oxidation of the cladding during the base irradiation. The new alloys (Zirlo, M5, MDA,..) were developed mainly to limit the clad oxidation and hydriding in order to enhance the clad resistance during the PCMI phase.

During the base irradiation, due to the radial thermal gradient existing in the cladding, the hydrogen diffuses towards the cold zones and accumulates in the outer part of the cladding beneath the zirconium oxide layer. Because of a low solubility limit in the Zircaloy (a few ppm at room temperature), hydrogen precipitates in the cladding as an outer hydride rim with possible creation of massive blisters if zirconia layer spallation had occurred during irradiation. These brittle zones created before the test can act as a preferential site for incipient crack nucleation and clad failure. It has been evidenced that at the beginning of the RIA transient some small cracks are nucleated in this outer part of the clad with large hydride concentration (see Fig. 2). The length of these incipient cracks is almost equal to the depth of the outer hydride dense zone in the cladding. After this primary brittle crack initiation, if the crack propagates in the ductile sound clad, the failure of the cladding will occur. Indeed, crack propagation in the inner ductile part of the clad without failure of the rod has never been observed. This secondary ductile propagation until clad failure was evidenced in several rod failures that occurred in the CABRI and NSRR reactors, see Fig. 3.

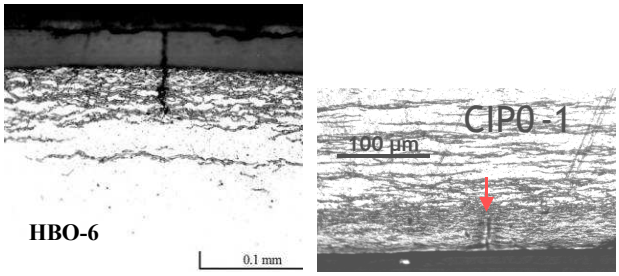

Fig. 2: metallographic examinations after HBO-6 and CIP0-1 tests.

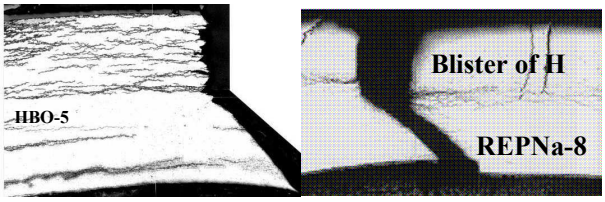

Fig. 3: metallographic examinations after HBO-5 and REPNa-8 tests.

The goal of the paper is to propose a fracture mechanics approach that gives the condition, during the PCMI phase, leading to propagation of these incipient brittle cracks in the sound clad until rod failure.

First, the fracture mechanics approach used to analyze the failure conditions is described. An analysis of the metallographic examinations before or after the transient is then performed on some CABRI and NSRR test rods to evaluate the depth of the brittle zone in the outer part of the cladding. For each test these experimental values are compared with calculated critical incipient cracks. Finally the results are analyzed and the differences between CABRI and NSRR reactor conditions are emphasized.

II. THE FRACTURE MECHANICS APPROACH USED WITH THE SCANAIR CODE

The stress intensity factor is commonly used to assess the integrity of a cracked component in the elastic range. The comparison between the stress intensity factor and the fracture toughness makes it possible to predict the behavior of a brittle material and had been already used for RIA tests interpretation ([7], [8]).

For materials loaded in the plastic range, the J-integral (also referred to as the Rice integral) provides an extension of linear elastic fracture mechanics to elastic-plastic fracture mechanics ([9]). The J-integral is a measurement of the loading intensity of a cracked structure in the elastic-plastic range. The Rice integral remains valid only for monotonously increasing loadings.

For irradiated cladding integrity assessment, a simple comparison to a critical J value is used in the present study:

- if $J < J_c$: the crack is considered to be stable,
- if $J \geq J_c$: the initial crack propagates in an unstable way.

The critical J value is derived from the cladding fracture toughness:

$$J_c = \frac{K_{Ic}^2 \left(1-\nu^2\right)}{E}. \qquad (1)$$

with K_{Ic}: fracture toughness, E: Young modulus and ν: Poisson ratio.

A survey of literature data was performed in order to derive fracture toughness values of irradiated Zircaloy-4 claddings. The literature review showed that the fracture toughness of irradiated claddings mainly depends on hydrogen content and cladding temperature. Dynamic influence on fracture toughness is not expected during RIA transients. We actually observed that quasi-static calculations performed in the SCANAIR code are in good agreement with experiments. Thus usual fracture toughness appears sufficient to describe the cladding failure and there is no need for dynamic fracture toughness. Among the set of relevant experiments ([10], [11] and [12]), data were used to determine a correlation giving fracture toughness

versus hydrogen content and cladding temperature (plotted in Fig. 4).

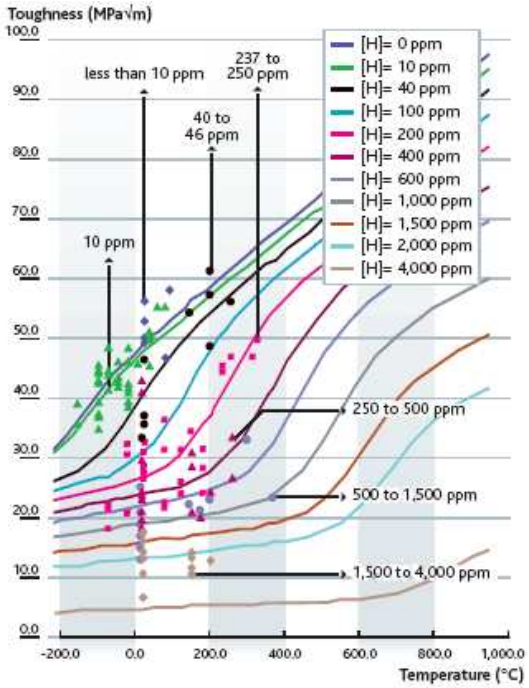

Fig. 4: Fracture toughness measurements and correlations vs. hydride concentration and temperature.

Regarding the J-integral calculation, it was decided to establish a tabulated dataset of J values determined with finite element calculations performed with the CAST3M computer code. The boundary conditions modelled in the finite element computations and typical aspect of the meshing close to the crack tip are illustrated in Fig. 5. The material is assumed to be homogeneous irradiated Zircaloy-4, no specific material properties were attributed to areas with hydride accumulation such as hydride lenses or hydride rims.

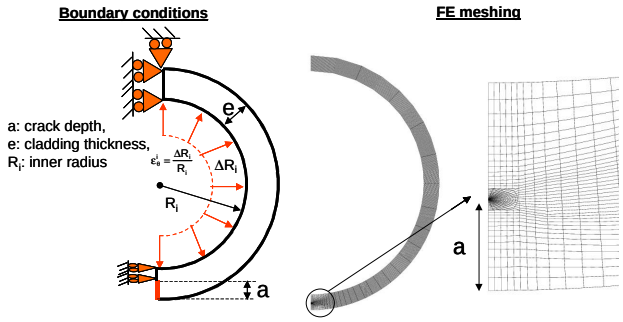

Fig. 5: Boundary conditions for J-integral calculations and CAST3M meshing

For a given cladding geometry with a given outer diameter crack depth, *a*, and a given cladding temperature, T, the J values are calculated by increasing the inner diameter radial displacement up to a maximum value. The imposed inner circumferential strain is derived by normalizing the controlled displacement by the cladding inner radius. Thus the J integral database depends on several parameters:

$$J = f\left(\frac{a}{e}; T; \varepsilon_\theta^i; R_i; e\right) \qquad (2)$$

An inner radius of 4.18 mm has been used in order to remain representative of 17x17 PWR assemblies with a 570 microns cladding thickness.
Three cladding thicknesses have been considered (respectively 470, 520 and 570 microns) in order to simulate the material consumption induced by primary water oxidation. A 520 microns cladding thickness corresponds to a 100 microns oxide layer thicknes. Five temperature levels ranging from room temperature up to 550°C and thirteen crack depths (a/e comprised between 0.07 up to 0.9) have been taken into account.

Plane strain conditions were assumed and elastic-plastic behaviour of irradiated Zircaloy-4 was modelled (see [13]). A typical evolution of the J integral with applied strain for several crack depths is illustrated in Fig. 6 at 350°C for a cladding thickness of 570 microns.

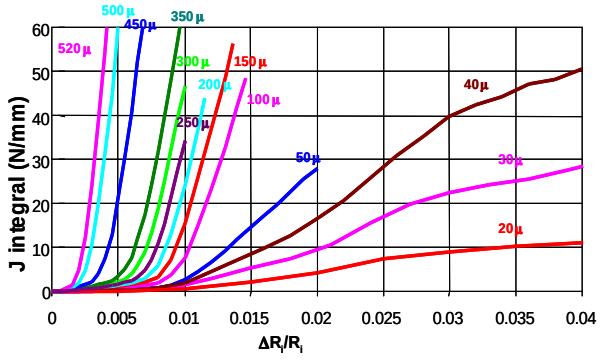

Fig. 6: J-integral as a function of crack depth and applied strain calculated by CAST3M at 350°C for a cladding thickness of 570 micrometers.

In order to establish the database, it was convenient to control the loading internal strain, but the outer strain and temperature better controls the cladding failure. For this reason, a parametric calculation of the outer diameter hoop strain versus the inner diameter hoop strain has been performed with CAST3M. This study shows that a very simple correlation can be easily applied and provides an accurate assessment of the hoop strain at the outer diameter of the cladding versus the inner hoop strain: $\varepsilon_\theta^e = 0.83.\varepsilon_\theta^i$. This relationship can be extended to any radial position, x, in the cladding:

$$\varepsilon_\theta^x = (1 - x/e)0.83.\varepsilon_\theta^i + x/e.\varepsilon_\theta^i . \quad (3)$$

The outer diameter failure strain of a cracked cladding is determined by solving:

$$f\left(\frac{a}{e}; T; \frac{\varepsilon_\theta^e}{0.83}; R_i; e\right) = J_C([H], T) \quad (4)$$

Alternatively, when the strain and temperature are calculated with a RIA code, it is possible to determine at each time step the crack depth that would induce failure. In other words

- the cladding will survive the transient only if it contains a crack shorter than the minimum calculated crack depth during the whole transient,
- the rod that fails under a RIA transient should contain a crack longer than the crack size calculated at the failure time.

The J integral is only defined for monotonously increasing loadings, this is not the situation during the whole RIA transient. Thus loading history is taken into account in the fracture mechanics analysis using simple rules. A time step is considered only if the current mechanical strain is greater than each of the past mechanical strains. Similarly only decreasing critical crack sizes are taken into account.

The proposed fracture mechanics analysis was implemented in SCANAIR ([14]).

A more detailed fracture prediction would require to model both Zircaloy-4 and the hydride dense area. But such a calculation would also require to determine the internal stresses induced by the specific volume of each material. These internal stresses are partly relaxed with creep under irradiation. It appeared to be excessively complex and authors decided to model homogenous but cracked materials.

III. RESULTS

The metallographic examinations performed before or after the tests have been analyzed to determine the brittle zone depth in the outer part of the cladding.

Two hypotheses have been considered

- the brittle zone is limited to the outer hydride ***rim or blister*** : zone where [H] is almost saturated (~16000ppm)
- the brittle zone is extended to all the "***dense hydride zone***": zone where the distance between adjacent hydrides is lower than 10 µm.

The results of these evaluations are gathered in TABLE I for non failed tests and TABLE II for failed tests. This method of brittle zone evaluation has a significant uncertainty because

- the metallographic examinations used for the analysis are not always representative of the clad microstructure. Indeed pre-test examinations are performed on the father rod at a different axial location with slightly different oxidation and hydriding compared to the tested rod and post-test examinations exhibit hydride distributions that may have been modified by the thermo-mechanical loading,
- the results may be linked to the number of metallographic examinations performed in the cladding. This is particularly the case for rods with axial heterogeneity as it is the case for initially spalled rods with hydride blister. As an example, on radial cuts performed after the REPNa-1 test, several hydride blisters have been observed but never thicker than 150µm, while it is most likely that blisters deeper than 300µm existed before the test in this rod, as observed in similar rods,
- there is also an uncertainty linked to the fact that the optical determination of the brittle limit may be subjective and then be "operator dependent".

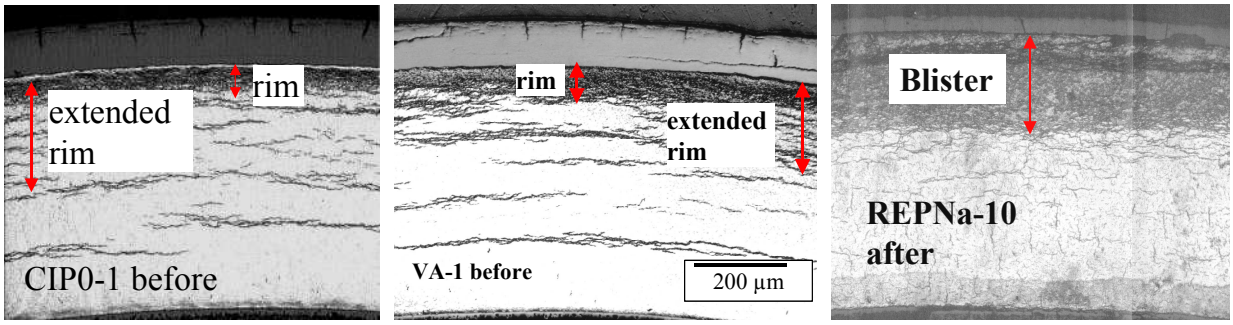

Fig. 7: Examples of brittle zone evaluation

For each test a SCANAIR calculation has been performed to evaluate the minimal size of critical crack for non failed cases and the size of critical crack at failure time for failed cases. The results calculations are gathered in TABLE I and TABLE II. The comparison between calculated critical cracks and evaluated brittle zone depth is presented on Fig. 8 and Fig. 9.

TABLE I
Non failed tests main characteristics and results

test	Clad /Burnup (GWd/tM)	Einjected/ Hmax (cal/g)	Brittle zone depth (µm)		Minimum Calculated critical crack (µm)
			Rim	Extended rim	
NSRR TESTS					
HBO-2	Zr-4 / 50.4	51/37	63	112	443
HBO-3	Zr-4 / 50.4	95/74	16	63	159
HBO-4	Zr-4 / 50.4	67/50	21	42	374
HBO-6	Zr-4 / 49	109/85	43	50	78
HBO-7	Zr-4 / 49	112/88	50	50	58
TK-3	Zr-4 / 50	126/99	32	32	56
TK-4	Zr-4 / 49.7	125/98	31	31	40
OI-10	MDA/60.2	138/104	47	47	40
OI-12	NDA/61	183/143	52	52	37
CABRI TESTS					
REPNa-3	Zr-4 / 52.8	122/123	30	100	50
REPNa-4	Zr-4 / 63	95/87	100	200	176
REPNa-5	Zr-4 / 65	104/108	10	20	88
REPNa-6	Zr-4 / 47	156/133	30	30	49
REPNa-9	Zr-4/28	233/197	0	20	61
CIP0-1	Zirlo/ 75	98/92	50	150	128
CIP0-2	M5 / 75	90/82	0	10	414

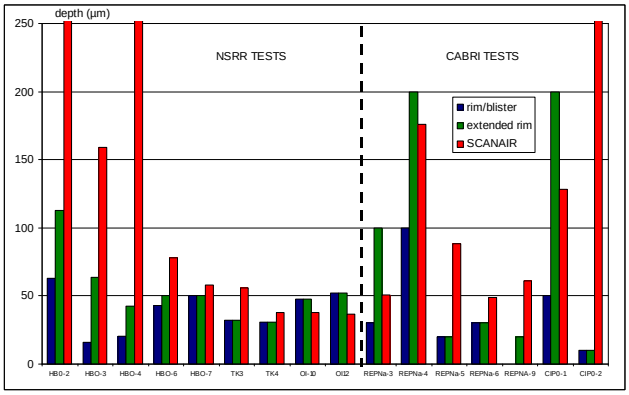

Fig. 8: comparison between minimal calculated minimum critical crack and measured brittle zone for non failed tests

Non failed tests : there is a rather good agreement between experimental observations and SCANAIR calculations: in almost all the tests the calculated critical crack is higher than the observed brittle zone depth (CABRI) or extended brittle zone (NSRR) in coherence with non failure of the rods. Nevertheless it should be noted that:

- in CABRI REPNa-3, REPNa-4 and CIP0-1 tests, the calculated critical crack is lower than the depth of the extended rim zone
- in NSRR OI-10 and OI-12 the critical crack is slightly lower than the depth of the brittle zone.

TABLE II
Failed tests main characteristics and results

Test	Clad /Burnup (GWd/tM)	Einjected / Hfailure (cal/g)	Brittle zone depth (µm)		Calculated critical crack at failure time (µm)
			Rim	Extended rim	
NSRR TESTS					
HBO-1	Zr-4 / 50.4	93/60	50	90	220
HBO-5	Zr-4 / 44	102/77	71	277	102
TK-2	Zr-4 / 48	136/60	70	120	250
TK-7	Zr-4 / 50	122/86	31	78	70
OI-11	Zirlo / 58.1	201/120	47	100	35
VA-1	Zirlo / 71	162/69	85	240	138
VA-2	MDA / 77	166/60	84	250	228
CABRI TESTS					
REPNa-1	Zr-4 /63.8	110/36	185	300	435
REPNa-7	Zr-4 / 50.4	170/113	50	50	89
REPNa-8	Zr-4 / 50.4	103/78	270	220	216
REPNa-10	Zr-4 / 50.4	108/81	190	210	210

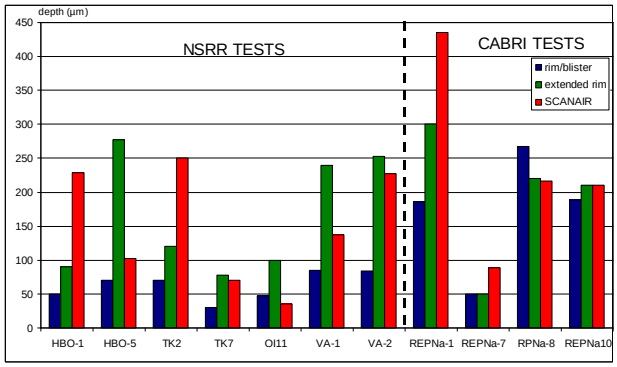

Fig. 9: comparison between minimal calculated critical crack and observed brittle zone for failed tests

Failed tests : in most of the cases the calculated critical crack length at failure time is smaller than the depth of the brittle zone (CABRI) or extended brittle zone (NSRR), but:

- for REPNa-1, the calculated critical crack depth is larger than the depth of the observed blister. As mentioned before, due the strong axial heterogeneity of clad hydride distribution linked to the initial zirconia spalling, it is likely that a large blister existed outside the few locations were metallographic examinations took place,
- for HBO-1 and TK-2 tests the calculated critical crack is larger than the observed brittle zone depth. The difference may be linked to the sampling of metallographic examinations or to experimental uncertainty (failure enthalpy,…).

IV. DISCUSSION

According to SCANAIR calculations, fuel rods with equivalent hydride distribution shall fail at a lower fuel enthalpy in the NSRR reactor than in the CABRI reactor. This phenomenon is evidenced by the comparison between CIP0-1 and VA-1 tests. Both rods were fabricated with similar cladding (Zirlo) irradiated up to close burnup and with similar zirconia thickness (~80µm) and hydride distribution (Hcontent: 800-1000ppm, rim: 50µm, extended rim: 200µm). Nevertheless, the VA-1 rod failed at a fuel averaged enthalpy of 69 cal/g while the CIP0-1 rod survived an enthalpy of 92 cal/g (*i.e.* an enthalpy increase of 75 cal/g).

To explain this phenomenon, it must be first quoted that the reactor test conditions are different, see Fig. 10. In CABRI, tests were performed with coolant sodium at 280°C while in NSRR reactor most of the test are performed with stagnant water at 20°C. Furthermore, while for the different tests in CABRI the pulse width at half maximum ranges between 10 and 80 ms, in NSRR it ranges between 4 and 10ms (all the failed tests mentioned in this paper were performed with 4 ms).

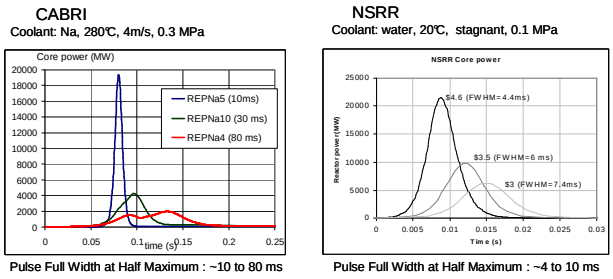

Fig. 10: comparison between CABRI and NSRR tests conditions.

These different tests conditions have an impact mainly on the clad temperature history during the PCMI phase of the transient. The comparison of calculated outer clad temperature evolutions during a CABRI transient and an NSRR transient as a function of enthalpy are plotted on Fig. 11.

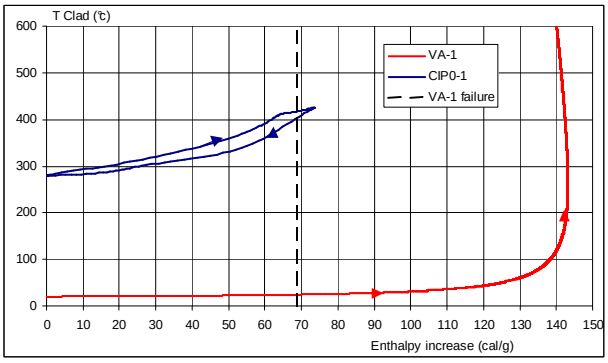

Fig. 11: Calculated outer clad temperature during VA-1 and CIP0-1 tests

At the failure time of VA-1, the temperature of the outer half of the clad was still close to the initial temperature of 20°C. On the contrary, in CIP0-1, the clad temperature rapidly reaches values above 400°C, because of the initial temperature of 280°C and the "large" (compared to VA-1) pulse width (30ms).

This temperature difference has an impact on the dissolved hydrogen content and therefore on the hydride precipitates in the clad during the test. Referring to curves defining hydrogen solubility limits versus temperature in zirconium alloys (see Fig. 12), one can evaluate that a hydrogen quantity comprised between 200 and 1000 ppm was dissolved during the CIP0-1 transient (consistent with the fact that a significant amount of radial hydrides were evidenced after the test, [2]).

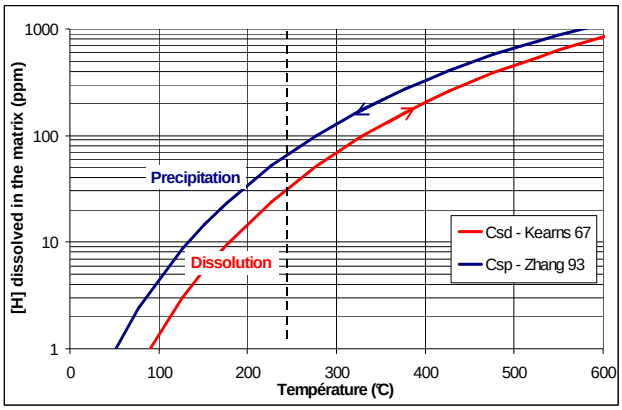

Fig. 12: hydrogen dissolution and precipitation diagram from [16], [17]

Consequently, apart from the ~50 µm outer rim, most of the hydrides were dissolved and vanished during the heat up phase in CIP0-1. On the contrary, at the time of failure of VA-1, negligible hydrogen dissolution had occurred in the outer part of the clad, see Fig. 13. In this situation, the VA-1 result indicates that the length to be compared to the critical crack size is not only the depth of the hydrogen rim but must also include the underlying zone containing significant hydrogen concentration, that is to say, the extended brittle zone.

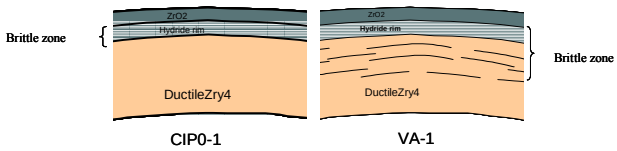

Fig. 13: Schematic representation of hydrides morphology at time of maximal mechanical loading Left: CIP0-1, right VA-1

V.SUMMARY AND CONCLUSIONS

This analysis shows that during the PCMI phase of a RIA transient a fracture mechanics approach using the J-integral evaluation can be applied both in the elastic and the elasto-plastic domains to predict the failure occurrence. The main difficulty is to determine the depth of the outer brittle zone in the cladding.

The study also shows that, due to the strong dependence of hydride solubility with temperature, the brittle zone is deeper at room temperature conditions than at PWR conditions. The incipient crack depth to be considered in NSRR tests is then not only the depth of the hydride rim in the cladding but also an underlying zone containing a significant hydrogen concentration. During PCMI phase, the NSRR testing conditions are thus more severe than the CABRI ones and than the ones expected in PWR cases.

The rim depth that should be evaluated in PWR cases can be deduced from the outer zirconia thickness of the cladding. This approach will then be used to derive a failure limit for zirconium based alloy during a RIA transient.

The interpretation of tests in the new high-temperature high-pressure capsule (70 bar, 280°C) in NSRR and in the future CABRI water loop (155 bar, 280°C) will make it possible to obtain test results in conditions more representative of PWR ones and to validate more accurately the methodology for the failure limit determination.

ACKNOWLEDGMENTS

The authors thank all the experimental teams from CABRI (IRSN and CEA) and NSRR (JAEA) who performed the tests and examinations.

REFERENCES

[1] J. Papin, B. Cazalis, J. M. Frizonnet, J. Desquines, F. Lemoine, V. Georgenthum, F. Lamare, M. Petit "*Summary and Interpretation of the CABRI REP-Na Program" Nuclear Technology* **Volume 157** Number 3 March 2007 Pages 230-250

[2] J. Papin, M. Petit, C. Grandjean and V. Georgenthum "*IRSN R&D studies on high burnup fuel behaviour under RIA and LOCA conditions" "* Proc of TOPFUEL 2006, Salamanque - Espagne, 22-26 octobre 2006

[3] T. Fuketa, T. Nakamura, K. Ishijima, "The Status of the RIA Test Program in the NSRR", Proc. 25th Water Reactor Safety Meeting, Bethesda, MD, Oct. 20-22, 1997, NUREG/CP 0162, Vol. 2, p. 179

[4] T. Sugiyama "*Results from recent RIA tests with high burnup fuels"* Fuel Safety Research Meeting 2006, Tokai, Japan, April 20-21, 2006

[5] T. Sugiyama *"PCMI failure of high burnup fuels under RIA conditions"* Proc of Fuel Safety Research Meeting 2007, Tokai, Japan, May 16-17, 2007

[6] T. Fuketa, F. Nagase, M. Suzuki and T. Sugiyama *"JAEA Studies on High Burnup Fuel Behaviors during Reactivity-Initiated Accident and Loss-of-Coolant Accident" "* Proc of the 2007 International LWR Fuel Performance Meeting, San Francisco, California, September 30 – October 3, 2007

[7] Y. Udagawa "*Stress Intensity Factor at the Tip of Cladding Incipient Crackunder RIA conditions*" Proc of Fuel Safety Research Meeting 2007, Tokai, Japan, May 16-17, 2007

[8] M. Kuroda, S. Yamanaka, F. Nagase, H. Uetsuka *"Analysis of the fracture behavior of hydrided fuel cladding by fracture mechanics"* Nuclear Engineering and Design 203 (2001) 185–194

[9] J.R. Rice "*A path independent integral and the approximate analysis of strain concentration by notches and cracks*", Journal of applied mechanics, pp. 379-386, 1968.

[10] T.J. Walker, J.N. Kass *"Variation of Zircaloy fracture toughness"* ASTM-STP 551, pp. 328-354, 1974.

[11] P.H. Kreyns, W.F. Bourgeois, C.J. White, P.L. Charpentier, B.F. Kammenzind, D.G. Franklin *"Embrittlement of core materials"*, ASTM-STP 1295, pp. 758-782, 1996.

[12] B. Watkins, A. Cowan, G.W. Parry, B.W. Pickles *"Embrittlement of Zircalo-2 pressure tubes",* ASTM-STP 458, pp. 141-159, 1969.

[13] B. Cazalis, J. Desquines, C. Poussard, M. Petit, Y. Monerie, C. Bernaudat, P. Yvon, X. Averty *"The PROMETRA program: fuel cladding mechanical behavior under high strain rate"*, Nuclear Technology, Vol.157, pp. 215-229, 2007.

[14] E. Federici, F. Lamare, V. Bessiron, J. Papin *"The SCANAIR Code Version 3.2: Main features and Status of Qualification", "* Proc of IAEA TCM on Fuel Behavior

Under Transient and LOCA Conditions, Halden, Norway, September 10-14, 2001

[15] M. Petit, V. Georgenthum, J. Desquines, T. Sugiyama; M. Quecedo *A comparative analysis of CABRI CIP0-1 and NSRR VA-2 Reactivity Initiated Accident tests* Proceedings of Eurosafe Meeting 2007, Berlin

[16] J.J.Kearns "Terminal solubility and partitioning of hydrogen in the alpha phase of zirconium, Zircaloy-2 and Zircaloy-4" Journal of Nuclear Materials – Vol.22 – pp.292-303 - 1967.

[17] J.H.Zhang "Hydruration du Zircaloy-4 et étude de la distribution de l'hydrogène dans une gaine de combustible REP"
CEA report -R-5634 – 1993